Paper No. DS1-T5-1, pp. 1-4

18th INTERNATIONAL SYMPOSIUM on POWER ELECTRONICS - Ee 2015

NOVI SAD, SERBIA, October 28th - 30th, 2015

FERRITE CORE LOSS MEASUREMENT ISSUES AND TECHNIQUE

Miodrag Milutinov, Nelu Blaz, Ljiljana Zivanov
University of Novi Sad, Faculty of Technical Sciences, Novi Sad, Serbia

Abstract: *Magnetic losses and permeabilities on commercial Mn-Zn ferrites 3F3 using a wattmeter method up to 2 MHz sinusoidal excitation is investigated. Digital oscilloscope with 50 Ohms input resistance is used to measure the sensing winding voltage and current sensor voltage. A new wattmeter method is analyzed to overcome the issue caused by low resistance instrument's input in sensing winding circuit. In order to validate new measurement procedures results are compared with manufacturer data sheet.*

Key Words: ***Magnetic loss/Wattmeter/Ferrite cores***

1. INTRODUCTION

Characterization of ferrite cores is important part in process of designing inductors. It is essential in selecting of proper core material. Ferrite materials are nonlinear which characteristics such as power loss, complex permeability, amplitude permeability depends on both, frequency and intensity of the magnetic field inside the core. It is proposed and developed a number of different methods for measuring these characteristics under sinusoidal and non-sinusoidal (DC biased) excitation using an impedance or network analyzer [1]-[5]. Review of existing core loss measurement technique based on wattmeter methods with their advantages and disadvantages are presented in [6]. Validation of proposed methods is usually tested on commercial Mn-Zn and Ni-Zn ring samples.

In this paper it is analyzed a core loss measurement setup based on digital oscilloscope DSO90604A Infiniium High Performance Oscilloscope (DSO) and function generator (FG) Voltcraft 7202 under sinusoidal excitation. Schematic of wattmeter method used in this paper is shown in Fig. 1. Validation of proposed methods is tested with 3F3 and 3E5 ring cores (Ferroxcube®) [7].

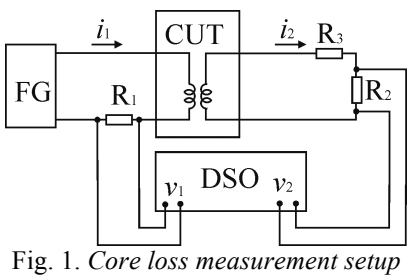

Fig. 1. *Core loss measurement setup*

The novelty in this setup are sensing resistor R_2 and series resistor R_3 placed in sensing winding circuit, which purpose will be explained in detail.

2. THEORETICAL APPROACH

The core under test (CUT) shown in Fig. 1, could be modeled as transformer with a magnetizing inductance L_m, and core resistance R_m connected in series, and placed on the primary side of transformer, as shown in Fig. 2. Core under test are wound with the same number of turns (N_1=N_2=N), as shown in Fig. 3. Function generator has output resistance of 50 Ω. Oscilloscope channels with input resistance of 50 Ω and passive probes (HP10437) are modeled as resistances R_{osc}.

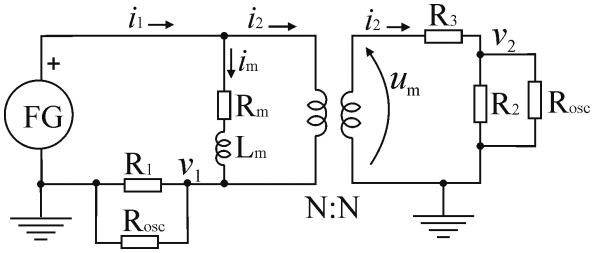

Fig. 2. *Model of CUT*

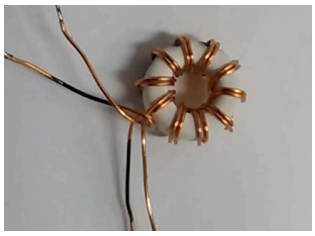

Fig. 3. *3F3 Ring core with bifilar winding*

Due to CUT has same number of turns with bifilar winding, the magnetizing current i_m, could be expressed by

$$i_m = (i_1 - i_2) = \left(\frac{v_1}{R_{e1}} - \frac{v_2}{R_{e2}}\right), \quad (1)$$

where v_1 and v_2 are measuring voltages, R_{e1} and R_{e2} are equivalent resistance obtained from sensing resistance R_1 and R_2 in parallel with R_{osc} respectively and l_e is effective length of toroid cores. Digital oscilloscope has ability to set input attenuation, which is used to control the

amplitude of applied magnetic field by setting the constants k_{ch1} and k_{ch2} determined by expression

$$k_{ch1} = N/(l_e R_{e1}),\ k_{ch2} = N/(l_e R_{e2}) \quad . \tag{2}$$

Magnetic field is monitored directly on the DSO applying the internal mathematical operation (3) on measured signals

$$H = \frac{N i_m}{l_e} = k_{ch1} v_1 - k_{ch2} v_2 , \tag{3}$$

The formulas for the induced voltage in secondary winding, magnetic flux density and core loss calculation are

$$u_m = \frac{(R_3 + R_{e2})}{R_{e2}} v_2 , \tag{4}$$

$$B = \frac{1}{NA_e}\int_0^T u_m \mathrm{d}t = \frac{1}{NA_e}\frac{(R_3 + R_{e2})}{R_{e2}}\int_0^T v_2 \mathrm{d}t \ , \tag{5}$$

$$P_{core} = \frac{1}{T}\int_0^T i_m u_m \mathrm{d}t \ , \tag{6}$$

where A_e is effective cross-sectional area of a core, T is the period of sinusoidal waveform. Dividing calculated core loss P_{core} by the effective core volume, V_e, we can obtain the core loss density.

One of major disadvantage of wattmeter method as described in [1] and mention in [6] is sensitivity to phase discrepancy between measuring voltages v_1 and v_2. In [6] is explained that if v_1 and v_2 have more than 87° phase difference, than 1° of phase discrepancy will produce core loss error more than 20%. This issue could be overcame by resonant capacitor method, or inductive cancellation method proposed in [6]. In measurement setup analyzed in [1]-[6] v_2 is voltage induced on sensing winding.

In our paper induced voltage is denoted by u_m and it is calculated using equation (4). Resistance R_3 and R_{e2} as part of measurement setup decreasing the phase difference between v_1 and v_2. For example, R_3 = 1 kΩ and R_2 = 50 Ω will reduce the phase difference from 87° to 84°. In that case for the same 1° of phase discrepancy core loss error will be reduced from 20% to 10%. Another source of phase discrepancy is oscilloscope sampling rate, but in case of 20 GSa/s on DSO90604A, it could be neglected.

Stray capacitances presented in transformer at high frequency is fully described in [8]. Stray capacitances between primary and secondary winding could be neglected due to same number of turns, which keep the voltage drop between windings close to zero. Serial winding resistances, leakage inductances and self-capacitances of primary and secondary winding are include in the model as parameters.

3. MEASURED RESULTS

The method described in previous section is tested on commercial ferrite cores 3F3 TN10/6/4, with l_e=24 mm, A_e=7.8 mm^2 and V_e=24 mm.

As a function generator (FG) the Voltcraft 7202 under sinusoidal excitation is used. Output impedance and maximum output voltage of FG are 50 Ω and 20Vpp.

Waveforms captured from oscilloscope is saved in *.csv format and processed by in house developed software, which Graphic User Interface (GUI) is shown in Fig. 4. Using this GUI it is possible to change any of parameters in the model or in the core in order to see their impact on final results. The software could include winding resistance and inductance due to skin effect, stray capacitance and leakage inductance.

Wire of the winding is modeled as copper wire which

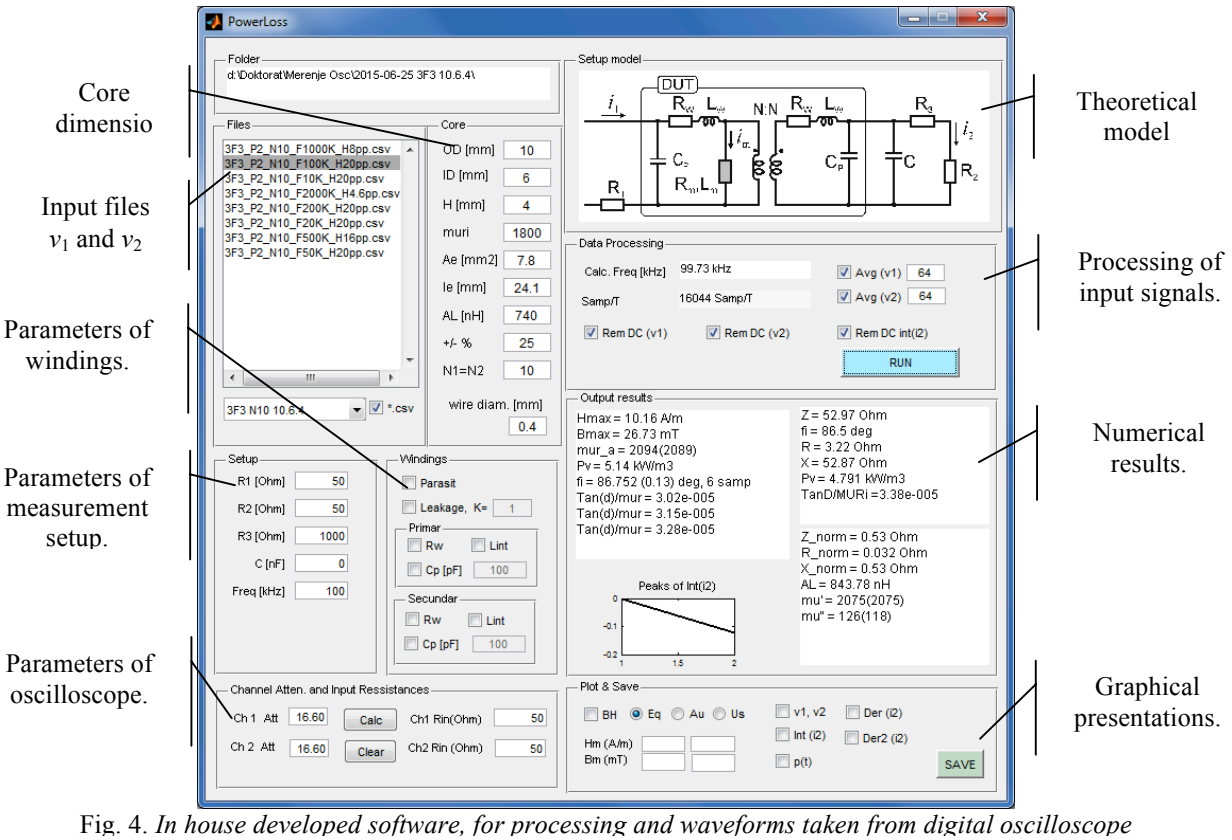

Fig. 4. *In house developed software, for processing and waveforms taken from digital oscilloscope*

diameter could be set trough GUI and length which is calculated automatically from core dimensions and number of turns. Wire AC resistance and AC internal inductance is calculated based on the skin effect taking into account the measuring frequency. Turning on/off this parameter and comparing results with available data sheet it could be concluded does this parameter could be neglected.

Winding leakage inductance $L_{leakage} = (1-k)L$ depends on coupling coefficient k and self-inductance L which is taken from manufacturer data sheet. It could be turn on/off with ability to manually set the value of parameter k. Stray capacitance could be turn on/off with ability to manually set the value. All of these three parameter which present parasitic effect could be set on primary and secondary windings.

Resistance R_1, R_2 and R_3 and capacitance C are part of measurement setup and their values could be manually set and changed. Ability of DSO of attenuation of the channel inputs and mathematical operations implemented in DSO is used to control the magnetic field inside the core according the equations (2) and (3). The attenuation constants k_{ch1} and k_{ch2} could be inserted manually and they are used to recalculated voltages v_1 and v_2.

Final results depend on processing of captured voltages v_1 and v_2. With described GUI it was possible to turn on or off any of parameters as well as change their values in order to see their impact to final results, which is given as numerical values and graphs. Averaging ability is useful to obtained clear and smooth curve of hysteresis loop. Calculation of phase difference between voltages v_1 and v_2 is carefully design to minimize phase discrepancy.

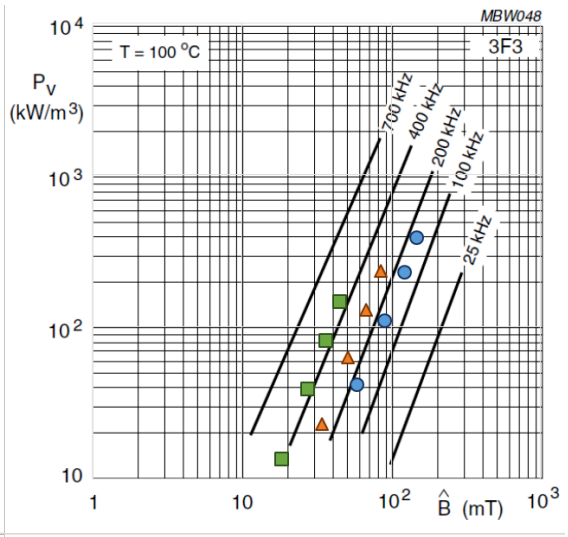

Fig. 5. *Specific power loss as a function of peak flux density. Markers present measured values (circles 100 kHz, triangles 200 kHz and squares 400 kHz). Solid lines are from manufacturer data sheet*

Increasing the value of the output voltage of FG from 2V to 10V in step of 2V and capturing waveforms v_1 and v_2 it is calculated both the magnetic flux density and specific power loss. Specific power loss as a function of peak flux density with frequency as a parameter is measured and compare to the available data sheet, as shown in Fig. 5. Measurements are perform at three different frequencies of 100 kHz, 200 kHz and 400 kHz.

Comparing results it could be noticed that specific power loss obtain by measurement is less than one given by manufacturer. The reason for disagreement is temperature dependence of power loss as shown in Fig. 6. The measurements was performed at temperature of 30°C and curves in data sheet are at temperature of $T = 100\,°C$.

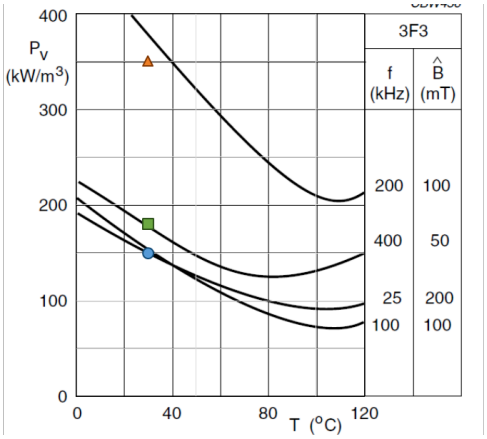

Fig. 6. *Specific power loss as a function of temperature obtained from data sheet*

To verify the method it was necessary to compare measured specific power loss with values from data sheet which correspond to the same temperature.

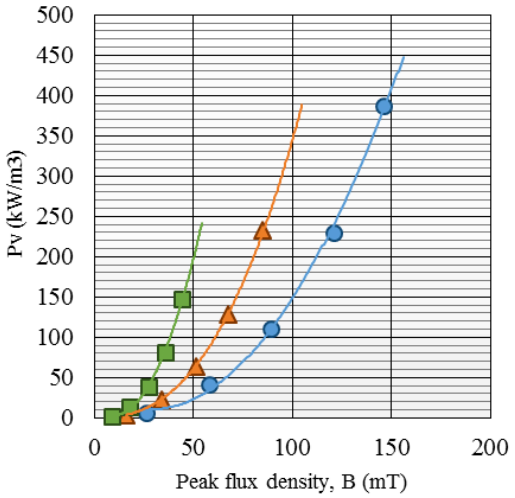

Fig. 7. *Specific power loss as a function of peak flux density at temperature of 30 °C. Markers present measured values and solid line are trend line*

Lines presented in Fig. 6 correspond only for several specific magnetic flux density which some of them are not reached by measurement. Therefore a trend line, based on five measured values, is generated and used to estimate specific power loss at these specific values of magnetic flux densities. Measured values of magnetic flux densities and specific power loss, five for each frequency, are presented in Fig. 7. Final results, shown in Fig. 6, where markers present measured values at

temperature of 30°C, are in satisfactory agreement with data sheet.

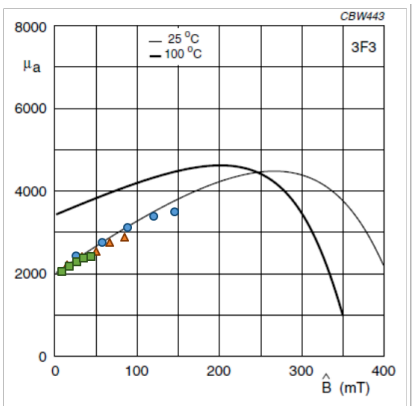

Fig. 7. *Amplitude permeability as a function of peak flux density. Data sheet - solid lines, measurement data - markers*

Another verification of the method is perform comparing measured amplitude permeability as a function of peak flux density with one given by manufacturer, as it presented in Fig. 7. Amplitude permeability is calculated by

$$\mu_a = \frac{1}{\mu_0} \cdot \frac{B_{peak}}{H_{peak}}, \tag{7}$$

as it is defined in [4]. Measurement results for magnetic flux density in range from 0 to 150 mT are in good agreement with manufacturer data sheet. Markers shown in Fig. 7, correspond to three measured frequencies; circles (100 kHz), triangles (200 kHz) and squares (400 kHz).

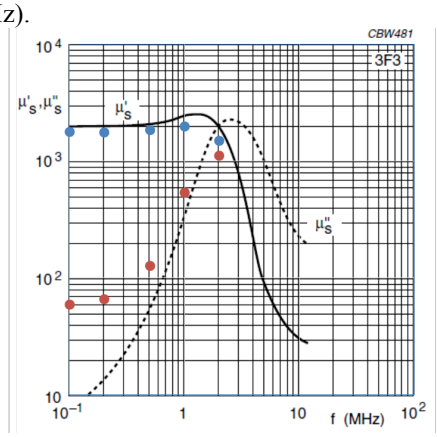

Fig. 8. *Complex permeability obtained by measurement (blue and read circles) and data sheet (black solid lines)*

Measurement setup with described software for processing captured waveform v_1 and v_2 is capable to measure complex permeability (8) as function of frequency with magnetic field as parameter.

$$\mu' = \frac{\mathrm{Im}\{\underline{Z}_m\}}{\omega \cdot L_0}, \quad \mu'' = \frac{\mathrm{Re}\{\underline{Z}_m\}}{\omega \cdot L_0} \tag{8}$$

$$\underline{Z}_m = \frac{\max(u_m)}{\max(i_m)} \cdot e^{\mathrm{j}S(u_m, i_m)} \tag{9}$$

Frequency of FG are changed from 100 KHz up to 2 MHz which is the maximum output frequency of the FG. Results are shown in Fig. 8. Real part of complex permeability is in good agreement. Disagreement of imaginary part of complex permeability is due to high value of magnetic flux density (above 20 mT) which increase the power loss. This lack of the method could be overcome using another FG with low output voltage and low noise to signal ratio.

4. CONCLUSION

A classic wattmeter method was changed and adjusted to the measurement setup which use 50 Ohm's input Oscilloscope. The method is tested on Mn-Zn ferrite core 3F3 in frequency range up to 2 MHz. In this frequency range results, obtained by new wattmeter method, show a good agreement with specific core loss given by the manufacturer. Measured results of amplitude permeability as a function of peak flux density in the range that we could achieve without an RF amplifier, are in satisfactory agreement with data sheet. Improving the method decreasing the noise it could be used to measure complex permeability as well. Further research will be directed in increasing the frequency range and testing the method on both the Mn-Zn and Ni-Zn ferrite ring cores.

ACKNOWLEDGEMENT

This work is supported by the Serbian Ministry of Education, Science and Technological Development under the grant for the project TR 32016.

5. REFERENCES

[1] F. Tan, J. Vollin, and S. Cuk, *"A Practical Approach for Magnetic Core-Loss Characterization"*, IEEE Trans. Power Electronics, vol. 10, No. 2 pp. 124-129, Mar. 1995.

[2] Ju Zhang, G. Skutt, F. Lee, "*Some practical issues related to core loss measurement using impedance analyzer approach"*, APEC '95, pp547-553, vol.2, Conference Proceedings 1995.

[3] Y. Han, W. Eberle and Y. Liu, *"New Measurement Methods to Characterize Transformer Core Loss and Copper Loss In High Frequency Switching Mode Power Supplies"*, 35th Annual IEEE Power Electronics Specialists Conference, Germany, 2004

[4] C. Baguley, U. Madawala and B. Carsten, "*A New Technique for Measuring Ferrite Core Loss Under DC Bias Conditions*" IEEE Trans. on Magnetics, Vol. 44, No. 11, November 2008.

[5] N. Blaz, A. Maric, G. Radosavljevic, L. Zivanov and G. Stojanovic, "*Modeling and characterization of frequency and temperature variation of complex permeability of ferrite LTCC material*", Progress In Electromagnetics Research B, vol. 23, pp. 131-146, 2010.

[6] Mingkai Mu: *High Frequency Magnetic Core Loss Study*, PhD Dissertation, Blacksburg, Virginia, Feb. 2013.

[7] Soft Ferrites and Accessories Data Handbook 2013, Ferroxcube ®, www.ferroxcube.com.

[8] Marian K. Kazimierczuk: *High-frequency magnetic components*, Wright State University, Dayton, Ohio, USA, © 2014, John Wiley & Sons, Ltd